

# Robust manipulation of electron spin coherence in an ensemble of singly charged quantum dots

A. Greulich, M. Wiemann, F. G. G. Hernandez,<sup>\*</sup> D. R. Yakovlev,<sup>†</sup> I. A. Yugova,<sup>‡</sup> and M. Bayer  
*Experimentelle Physik II, Universität Dortmund, D-44221 Dortmund, Germany*

A. Shabaev<sup>§</sup> and Al. L. Efros  
*Naval Research Laboratory, Washington, DC 20375, USA*

D. Reuter and A. D. Wieck  
*Angewandte Festkörperphysik, Ruhr-Universität Bochum, D-44780 Bochum, Germany*  
 (Received 7 May 2007; published 6 June 2007)

Using the recently reported mode-locking effect [A. Greulich *et al.*, *Science* **313**, 341 (2006)], we demonstrate a highly robust control of electron spin coherence in an *ensemble* of (In,Ga)As quantum dots during the single spin coherence time. The spin precession in a transverse magnetic field can be fully controlled up to 25 K by the parameters of the exciting pulsed laser protocol such as the pulse train sequence, leading to adjustable quantum beat bursts in Faraday rotation. Flipping of the electron spin precession phase was demonstrated by inverting the polarization within a pulse doublet sequence.

DOI: 10.1103/PhysRevB.75.233301

PACS number(s): 78.47.+p, 72.25.Dc, 72.25.Rb, 78.55.Cr

The spin of an electron in a quantum dot (QD) is an attractive quantum bit candidate<sup>2-5</sup> due to its favorable coherence properties.<sup>1,6-8</sup> As the interaction strength is rather small for direct spin manipulation, the idea to swap spin into charge has been furbished.<sup>6,9,10</sup> For example, the electron may be converted into a charged exciton by optical injection of an electron-hole pair,<sup>10</sup> depending on the residual electron's spin orientation, leading to distinctive polarization selection rules.

The fundamental quantity regarding spin coherence is the transverse relaxation time  $T_2$ . In a QD ensemble, this time is masked by dephasing, mostly caused by dot-to-dot variations of the spin dynamics. The dephasing time does not exceed 10 ns, much shorter than  $T_2$ . This leads to the general belief that manipulations ought to be performed on a single spin. Measurement of a single electron spin polarization, however, also results in dephasing due to temporal sampling of varying nuclear spin configurations,<sup>11,12</sup> as statistically significant measurements on a single QD may require multiple repetition of the experiment. The dephasing can be overcome by spin-echo techniques, which give a single electron spin coherence time on the scale of microseconds.<sup>8</sup> This long coherence time derived by spin echo is the result of a refocusing of the electron spin and possibly the nuclear spin configuration,<sup>11</sup> and it is viewed as an upper bound on the free-induction decay of spin coherence.<sup>11,13</sup>

Recently, however, we have shown that mode locking of electron spin coherence allows one to overcome the ensemble dephasing<sup>14</sup> and to measure the single electron spin relaxation time  $T_2$  without applying spin-echo refocusing.<sup>1</sup> For monitoring the coherence, pump-probe Faraday rotation (FR) measurements<sup>15</sup> on a QD ensemble were used: after optical alignment of the spins normal to an external magnetic field, the electron spins precess about this field. Due to precession frequency variations, the ensemble phase coherence is quickly lost. However, a periodic train of circularly polarized pulses emitted by a mode-locked laser synchronizes those spin precession modes, for which the precession frequency is a multiple of the laser repetition rate. This synchronization leads to constructive interference (CI) of these

modes in the ensemble spin polarization before arrival of each pump pulse (see Fig. 1, upper left trace). The limit for spin mode locking is set by the single electron spin coherence time, which can last up to a few microseconds,<sup>1</sup> reaching the low bound on echolike decays.<sup>16</sup>

Here, we develop a detailed understanding of the degree of control, which can be reached for the electron spin coherence in an ensemble of singly charged QDs by exploiting the mode locking. For this purpose, trains of excitation pump pulse doublets were designed to vary the phase synchronization condition (PSC) for electron spin precession frequencies. The PSC selects a QD subset, whose contribution to the ensemble spin polarization shows a well controlled phase recovery. Variation of the pulse separation results in tunable patterns of quantum oscillation bursts in time-resolved FR, in good agreement with our calculation, which rely on a newly developed theoretical model. This tailoring of electron spin coherence is very robust, as the spin mode locking is stable up to 25 K. For higher temperatures, the coherence amplitude decreases due to phonon-assisted scattering of holes during the laser pulse excitation by which the spin coherence is created.

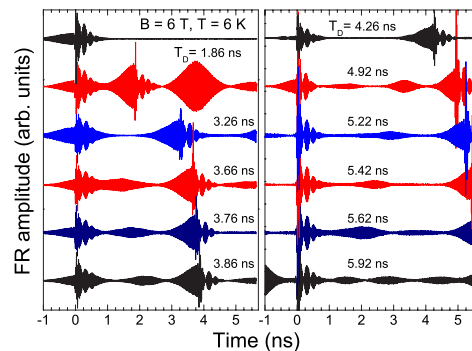


FIG. 1. (Color online) Faraday rotation traces measured as function of delay between probe and first pump pulse at time zero. A second pump pulse was applied, delayed relative to the first one by  $T_D$ , indicated at each trace. The top left trace gives the FR without second pump.

The studied self-assembled (In,Ga)As/GaAs QDs were fabricated by molecular beam epitaxy on a (001)-oriented GaAs substrate. The sample contains 20 QD layers with a layer dot density of about  $10^{10} \text{ cm}^{-2}$ , separated by 60 nm wide barriers.<sup>17</sup> For average occupation by a single electron per dot, the structures were  $n$ -modulation doped 20 nm below each layer with a Si-dopant density matching roughly the dot density. The sample was held in the insert of an optical magnetocryostat, allowing temperature variation from  $T=6$  to 50 K.

FR with picosecond time resolution was used for studying the spin dynamics: Thereby, spin polarization along the growth direction ( $z$  axis) is generated by a circularly polarized pump pulse hitting the sample along  $z$ , and its precession in a transverse magnetic field  $B \leq 7$  T along the  $x$  axis is tested by the rotation of the linear polarization of a probe pulse. For optical excitation, a Ti-sapphire laser was used, emitting pulses with a duration of  $\sim 1.5$  ps (full width at half maximum of  $\sim 1$  meV) at 75.6 MHz repetition rate (corresponding to a repetition period  $T_R=13.2$  ns). The laser energy was tuned into resonance with the QD ground state transition, and the laser pulses were split into pump and probe. The pump beam was split further into two pulses with variable delay  $T_D$  in between. The circular polarization of the two pumps could be controlled individually. For detecting the rotation angle of the probe beam linear polarization, a homodyne technique was used.

Figure 1 shows FR traces excited by the two-pulse train with a repetition period  $T_R=13.2$  ns, in which both pulses have the same intensity and polarization, and the delay between these pulses  $T_D$  was varied between  $\sim T_R/7$  and  $\sim T_R/2$ . The FR pattern varies strongly for the case when the delay time  $T_D$  is commensurate with the repetition period  $T_R$ :  $T_D=T_R/i$ , with  $i=2,3,\dots$ , and for the case  $T_D \neq T_R/i$ . For commensurability  $T_D=T_R/i$ , the FR signal shows strong periodic bursts of quantum oscillations only at times equal to multiples of  $T_D$ , as seen in the left panel of Fig. 1 for  $T_D=1.86$  ns  $\approx T_R/7$ . Commensurability is also given to a good approximation for delays  $T_D=T_R/4 \approx 3.26$  ns and  $T_D=T_R/3 \approx 4.26$  ns.

For incommensurability of  $T_D$  and  $T_R$ ,  $T_D \neq T_R/i$ , the FR signal shows bursts of quantum oscillations between the two pulses of each pump doublet, in addition to the bursts outside of the doublet. For example, one can see a single burst in between the pumps for  $T_D=3.76$  and 5.22 ns. Two bursts, each equidistant from the closest pump and also equidistant from one another, appear at  $T_D=4.92$  and 5.62 ns. Three equidistant bursts occur at  $T_D=5.92$  ns. Note also that the FR amplitude before the second pump arrival is always significantly larger than before the first pump for any  $T_D$ .

Although the time dependencies of the FR signal look very different for commensurate and incommensurate  $T_D$  and  $T_R$ , in both cases they can be fully controlled by designing the synchronization of electron spin precession modes in order to reach CI of their contributions to the FR signal.<sup>1</sup> A train of circularly polarized pump pulse singlets synchronizes those spin precessions for which the precession frequency satisfies the PSC:<sup>1,18</sup>  $\omega_e=2\pi N/T_R$ . Then the electron spin undergoes an integer number,  $N \gg 1$ , of full  $2\pi$  rotations in the interval  $T_R$  between the pump pulses.

For a train of pump pulse doublets, the PSC has to be extended to account for the intervals  $T_D$  and  $T_R-T_D$  in the laser excitation protocol,

$$\omega_e = 2\pi NK/T_D = 2\pi NL/(T_R - T_D), \quad (1)$$

where  $K$  and  $L$  are integers. On first glance, this condition imposes severe limitations on the  $T_D$  values, for which synchronization is obtained:

$$T_D = [K/(K+L)]T_R, \quad (2)$$

which for  $T_D < T_R/2$  leads to  $K < L$ . When Eq. (2) is satisfied, the contribution of synchronized precession modes to the average electron spin polarization  $\bar{S}_z(t)$  is proportional to  $-0.5 \cos[N(2\pi Kt/T_D)]$ . Summing over all relevant oscillations leads to CI of their contributions with a period  $T_D/K$  in time.<sup>1</sup> The rest of the QDs does not contribute to  $\bar{S}_z(t)$  at times longer than the ensemble dephasing time. The PSC Eq. (1) explains the position of all bursts in the FR signal for commensurate and incommensurate ratios of  $T_D$  and  $T_R$ . For commensurability,  $K \equiv 1$  and  $T_D = T_R/(1+L)$  according to Eq. (2). In this case, CIs should occur with period  $T_D$  as seen in Fig. 1 for  $T_D=1.86$  ns ( $L=6$ ).

For incommensurability of  $T_D$  and  $T_R$ , the number of FR bursts between the two pulses within a pump doublet and the delays at which they appear can be tailored. There should be just one burst between the pulses, when  $K \equiv 2$ , because then the CI must have a period  $T_D/2$ . A single burst is seen in Fig. 1 for  $T_D=3.76$  and 5.22 ns. The corresponding ratios  $T_D/T_R$  are 0.285 and 0.395, respectively. At the same time, Eq. (2) gives a ratio  $T_D/T_R=2/(L+2)$ , which is equal to 0.285 and 0.4 for  $L=5$  and 3, respectively, in good accord with experiment.

Next, two FR bursts are seen for  $T_D=4.92$  and 5.62 ns, corresponding to  $T_D/T_R \approx 0.372$  and 0.426. The corresponding CI period  $T_D/3$  is reached for  $K \equiv 3$ . Then from Eq. (2),  $T_D/T_R=3/(L+3)$ , giving 0.375 and 0.429 for  $L=5$  and 4, respectively. Finally, the FR signal with  $T_D=5.92$  ns ( $T_D/T_R \approx 0.448$ ) shows three FR bursts between the two pumps. The CI period  $T_D/4$  is obtained for  $K \equiv 4$ , for which Eq. (2) gives  $T_D/T_R=4/(L+4) \approx 0.444$  with  $L=5$ . Obviously, good general agreement between experiment and theory is established, highlighting the high flexibility of the laser protocol. In turn, this understanding can be used to induce FR bursts at wanted delays  $T_D/K$ , so that at these times further coherent manipulation of all electron spins involved in the burst is facilitated.

However, the question arises as to how accurate condition Eq. (2) for the  $T_D/T_R$  ratio must be fulfilled to reach phase synchronization. Formally, one can find, for any arbitrary  $T_D/T_R$ , large  $K$  and  $L$  values such that Eq. (2) is satisfied with high accuracy. However, the above analysis shows that only the smallest of all available  $L$  leads to PSC matching. Experimentally, the facilities to address this point are limited, as the largest  $T_D$  for which FR signal can be measured are delays around 5 ns between the two pumps. For larger delays, the FR bursts shift out of the scanning range. For short  $T_D$ , on the other hand, the bursts overlap with the FR signal from the pump pulses.

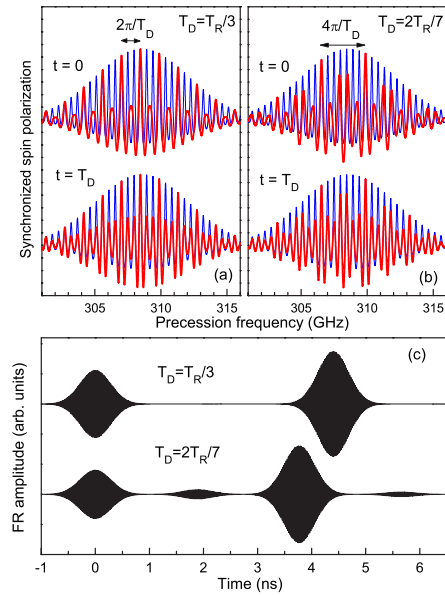


FIG. 2. (Color online) [(a) and (b)] Spectra of electron spin precession modes,  $-\tilde{S}_z(t)$ , which are phase synchronized by the two-pulse train calculated for  $T_D = T_R/3$  and  $T_D = 2T_R/7$  at the moments of first ( $t=0$ ) and second ( $t=T_D$ ) pulse arrivals [red (black)]. Single-pump spectra are shown in blue (gray). (c) FR traces calculated for two ratios of  $T_D/T_R$ . Laser pulse area  $\Theta = \pi$ .  $T_R = 13.2$  ns. Electron  $g$ -factor  $|g_e| = 0.57$  and its dispersion  $\Delta g = 0.005$ .  $B = 6$  T.

To answer this question, we have modeled the FR signal for commensurate and incommensurate ratios of  $T_D$  and  $T_R$ . Figure 2 shows the results, together with spectra of synchronized spin precession modes (SSPMs) at the moment of the first and second pump pulse arrivals. The SSPMs were calculated similar to those induced by a single pulse train.<sup>1</sup> Figure 2(a) gives the SSPM for commensurate  $T_D = T_R/3$  superimposed on the SSPM created by a single pulse train with the same  $T_R$ . Figure 2(c) shows the FR signal created by such a two-pulse train. The SSPMs for the considered strong excitation are considerably broadened and contain modes for which  $\omega_e = 2\pi M/T_D = 2\pi 3M/T_R$  with integer  $M$ , which coincide with each third mode created by a single-pulse train. However, the SSPMs given by  $\omega_e = 2\pi N/T_R$ , which do not satisfy the PSC for a two-pulse train, are not completely suppressed, because the train synchronizes the electron spin precession in some frequency range around the PSC. One sees also that at  $t=0$  the two-pulse train leads to a significant alignment of electron spins opposite to the direction of spins satisfying the PSC. This “negative” alignment decreases the CI magnitude and therefore the FR signal before the first pulse arrival, and is also responsible for a significantly larger magnitude of the FR signal before the second pulse arrival [see Figs. 1 and 2(c)].

For incommensurate ratios of  $T_D$ , and  $T_R$ , the SSPMs become much more complex. Still we are able to recover the modes which satisfy the PSC at the pulse arrival times. In Fig. 2(b), we show the SSPM at  $t=0$  and  $t=T_D$  for  $T_D = 2T_R/7$  ( $K=2$ ,  $L=5$ ), where the arrows indicate the frequencies which satisfy the PSC for the two-pulse train. Only a small number of such modes fall within the average distri-

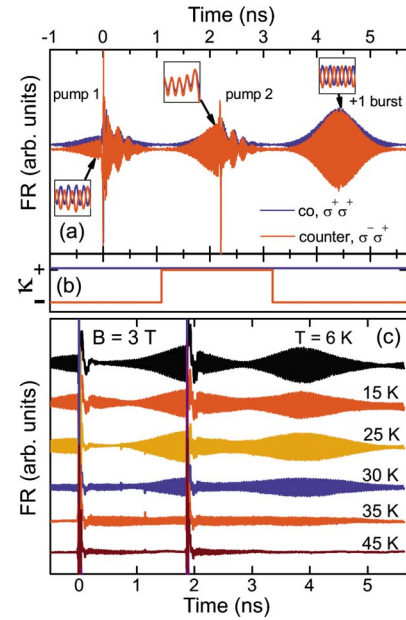


FIG. 3. (Color online) (a) Faraday rotation traces in the cocircularly [blue (black) traces] or countercircularly [red (gray) traces] polarized two-pump-pulse experiments measured for  $T_D = 2.2$  ns and  $B = 6$  T. Insets give close-ups showing the relative sign  $\kappa$  of the FR amplitude between the two traces.  $\kappa$  is plotted in (b) vs time. (c) Effect of temperature on the FR amplitude in two-pump-pulse experiment.  $T_D = 1.88$  ns.

tribution of electron spin precession modes, because the distance between the PSC modes is proportional to  $2\pi K/T_D = 2\pi(K+L)/T_R$ . The diluted spectra of PSC modes for incommensurability decrease the magnitude of the FR bursts between the pump pulses, in accord with experiment. This shows that, although any ratio of  $T_D/T_R$  can be satisfied by large  $K$  and  $L$ , the FR signal between the pulses should be negligibly small in this case. Consequently, not any ratio of  $T_D/T_R$  leads to pronounced FR bursts.

To obtain further insight into the tailoring of electron spin coherence, which can be reached by a two-pulse train, we have turned from co- to countercircularly polarized pumps. The delay between pumps  $T_D$  was fixed at  $T_R/6 \approx 2.2$  ns. The time dependencies of the corresponding FR signals are similar, as shown in Fig. 3. Besides the two FR bursts directly connected to the pump pulses, one sees a burst +1 due to CI of spin synchronized modes. The insets in Fig. 3(a) show close-ups of the different FR bursts. The sign  $\kappa$  of the FR amplitude for the countercircular configuration undergoes  $2T_D$ -periodic changes in time relative to the cocircular case, as seen in Fig. 3(b), which demonstrates optical switching of the electron spin precession phase by  $\pi$  in an ensemble of QDs.

The observed effect of sign reversal is well described by our model. Let us consider first a two-pulse train with delay time  $T_D = T_R/2$ , for which the two pumps are countercircularly polarized. In this case, an electron spin can be synchronized only if at the moment of pulse arrival, it has an orientation opposite to the orientation at the previous pulse. This leads to the PSC  $\omega_e = 2\pi(N+1/2)/T_D$ . The con-



tribution of such precession modes to the electron spin polarization is proportional to  $\cos[(2\pi(N+1/2)t/T_D)] = \cos(2\pi Nt/T_D)\cos(\pi t/T_D) - \sin(2\pi Nt/T_D)\sin(\pi t/T_D)$ . Summing these contributions, only the first term gives a CI, whose modulus has period  $T_D$ , while the sign of  $\cos(\pi t/T_D)$  changes with period  $2T_D$ . Only each third of the precession frequencies can be synchronized by a countercircularly polarized two-pulse train when the delay time is  $T_R/6$ , as in our experiment. However, the corresponding PSC has the same dependence on  $T_D$ . The CI modulus also has period  $T_D$  and its sign changes with period  $2T_D$ . The relative sign of the FR amplitude for the counter- and cocircularly case,  $\kappa = \text{sgn}[\cos[\pi t/T_D]]$ , is in accord with the experimental dependence in Fig. 3(b).

The CIs of the electron spin contributions can be seen only as long as the coherence of the electron spins is maintained. In this respect, the temperature stability of the CI is especially important. Figure 3(c) shows FR traces in a two-pump-pulse configuration with  $T_D=1.88$  ns at different temperatures. For both positive and negative delays, the FR amplitude at a fixed delay is about constant for temperatures up to 25 K, irrespective of slight variations which might arise from changes in the phase synchronization of QD subsets. Above 30 K, a sharp drop occurs, which can be explained by thermally activated destruction of the spin coherence.

The electron spin coherence in charged QDs is initiated by generation of a superposition of an electron and a charged exciton state by resonant pump pulses.<sup>17,19</sup> The simultaneous decrease of the FR magnitude before each pump pulse and afterward (when the CI signal is controlled by the excitation

pulse) suggests that the coherence at elevated temperatures is lost already during its generation. The 30 K temperature threshold corresponds to an activation energy of  $\sim 2.5$  meV. This energy may be assigned only to the splitting between the two lowest confined hole levels, because the electron level splitting dominates the 20 meV splitting between  $p$ - and  $s$ -shell emissions in photoluminescence and is much larger than 2.5 meV. The decoherence of the hole spin results from two-phonon scattering, which is thermally activated and should occur on a subpicosecond time scale, i.e., within the laser pulse.<sup>20</sup> The fast decoherence of the hole spin at  $T > 30$ K suppresses the formation of the electron-trion superposition state. Picosecond pulses as used here are therefore not sufficiently short for initialization of the superposition and creation of a long-lived electron spin coherence.

In summary, we have demonstrated that the mode-locking effect allows a far-reaching control of electron spin coherence in QD ensembles during the spin coherence time of microseconds.<sup>1</sup> Two-pulse train mode locking selects QD subsets which give a nondephasing contribution to the ensemble spin precession. The technique shows remarkable stability with respect to temperature increase up to 25 K, a property which is important for utilizing it in quantum information processing. The robustness of this control technique is provided by the dispersion of the spin precession frequencies in the QD ensemble.

This work was supported by the BMBF program nanoquit, the DARPA program QuIST, the ONR, the DFG (FOR485), and the FAPESP.

\*On leave from the Instituto de Física Gleb Wataghin, Campinas, SP, Brazil.

†Also at Ioffe Physico-Technical Institute, 194021, St. Petersburg, Russia.

‡Also at Institute of Physics, St. Petersburg State University, 198504, St. Petersburg, Russia.

§Also at School of Computational Sciences, George Mason University, Fairfax, VA 22030.

<sup>1</sup>A. Greilich *et al.*, *Science* **313**, 341 (2006).

<sup>2</sup>D. Loss and D. P. DiVincenzo, *Phys. Rev. A* **57**, 120 (1998).

<sup>3</sup>A. Imamoglu, D. D. Awschalom, G. Burkard, D. P. DiVincenzo, D. Loss, M. Sherwin, and A. Small, *Phys. Rev. Lett.* **83**, 4204 (1999).

<sup>4</sup>*Semiconductor Spintronics and Quantum Computation*, edited by D. D. Awschalom, D. Loss, and N. Samarth (Springer-Verlag, Heidelberg, 2002).

<sup>5</sup>S. M. Clark, K.-M. C. Fu, T. D. Ladd, and Y. Yamamoto, arXiv:quant-ph/0610152 (unpublished).

<sup>6</sup>J. M. Elzerman, R. Hanson, L. H. Willems van Beveren, B. Witkamp, L. M. K. Vandersypen, and L. P. Kouwenhoven, *Nature (London)* **430**, 431 (2004).

<sup>7</sup>M. Kroutvar, Y. Ducommun, D. Heiss, M. Bichler, D. Schuh, G. Abstreiter, and J. J. Finley, *Nature (London)* **432**, 81 (2004).

<sup>8</sup>J. R. Petta, A. C. Johnson, J. M. Taylor, E. A. Laird, A. Yacoby, M. D. Lukin, C. M. Marcus, M. P. Hanson, and A. C. Gossard, *Science* **309**, 2180 (2005).

<sup>9</sup>See, for example, R. Hanson, L. H. Willems van Beveren, I. T. Vink, J. M. Elzerman, W. J. M. Naber, F. H. L. Koppens, L. P. Kouwenhoven, and L. M. K. Vandersypen, *Phys. Rev. Lett.* **94**, 196802 (2005).

<sup>10</sup>See, for example, T. Calarco, A. Datta, P. Fedichev, E. Pazy, and P. Zoller, *Phys. Rev. A* **68**, 012310 (2003); P. Chen, C. Piermarocchi, L. J. Sham, D. Gammon, and D. G. Steel, *Phys. Rev. B* **69**, 075320 (2004).

<sup>11</sup>W. Yao, R. B. Liu, and L. J. Sham, *Phys. Rev. B* **74**, 195301 (2006).

<sup>12</sup>R. B. Liu, S. E. Economou, L. J. Sham, and D. G. Steel, *Phys. Rev. B* **75**, 085322 (2007).

<sup>13</sup>W. A. Coish, V. N. Golovach, J. C. Egues, and D. Loss, *Phys. Status Solidi B* **243**, 3658 (2006).

<sup>14</sup>For a general treatment on suppression of phase noise, see A. G. Kofman and G. Kurizki, *Phys. Rev. Lett.* **93**, 130406 (2004).

<sup>15</sup>J. M. Kikkawa and D. D. Awschalom, *Science* **287**, 473 (2000).

<sup>16</sup>R. Hanson, L. P. Kouwenhoven, J. R. Petta, S. Tarucha, and L. M. K. Vandersypen, arXiv: cond-mat/0610433, *Rev. Mod. Phys.* (to be published).

<sup>17</sup>A. Greilich *et al.*, *Phys. Rev. Lett.* **96**, 227401 (2006).

<sup>18</sup>A. Shabaev, Al. L. Efros, D. Gammon, and I. A. Merkulov, *Phys. Rev. B* **68**, 201305(R) (2003).

<sup>19</sup>T. A. Kennedy, A. Shabaev, M. Scheibner, Al. L. Efros, A. S. Bracker, and D. Gammon, *Phys. Rev. B* **73**, 045307 (2006).

<sup>20</sup>T. Takagahara, *Phys. Rev. B* **62**, 16840 (2000).